KINETICS OF AMMONIA OXIDATION ON COBALT CATALYST II APPLICATION OF TUBULAR REACTOR WITH CATALYTICALLY ACTIVE WALL

Bohumil BERNAUER, Antonín ŠIMEČEK and Jan VOSOLSOBĚ

Department of Inorganic Technology,
Prague Institute of Chemical Technology, 166 29 Prague 6

Received June 25th, 1980

The kinetics of ammonia oxidation on cobalt catalyst is described on basis of experimental data measured in the tubular reactor with catalytically active wall. In the temperature range up to 623 K, where the products of ammonia oxidation are nitrogen monoxide and elementary nitrogen, it is possible to describe the rate of formation of these components by empirical equations (*5*) and (*6*), at the temperature above 900 K, where the products are nitrogen dioxide and elementary nitrogen, by equations (*7*) and (*8*).

Catalytic ammonia oxidation is the only industrial source of nitric acid. As the catalyst is nearly exclusively used the alloy of platinum and rhodium in the form of meshes[1]. In the pressure process (0·4 to 0·8 MPa) which is advantageous with regard to better absorption of NO_x account the irreversible losses in the catalyst to 0·1 to 0·2 g/t HNO_3. In this way becomes this process, which enables to decrease the content of NO_x in the stack gases from absorption below 0·05 mol % (ref.[1]), considerably economically handicapped in comparison to processes performed at normal pressure. Therefore, there is from the time of introduction of catalytic ammonia oxidation into industrial application searched an equivalent substitute of the precious platinum catalyst. Together with this aim many scientists have tried to describe the feasible mechanism of ammonia oxidation both on platinum and oxidic catalysts[2–35].

Due to expansion of new experimental techniques have been only recently, at least, partially explained the questions concerning the structure of surface complexes and of the kinetics of their transformation[18–35]. The common sign of these methods is that the experiments are performed under low pressures ($10-10^{-3}$ Pa) or at lower temperatures (up to 400 K) and almost, exclusively on the Pt catalyst. The question remains whether it is possible under conditions of industrial exploitation (0·8 MPa, 1 100 K) to consider, the same mechanism which had been determined under considerably different conditions.

The aim of this study has been to obtain experimental data enabling, on basis of the two-dimensional model of the tubular reactor with the catalytically active wall proposed in the last study[36], and explanation of the concentration and temperature conditions on the surface of the cobalt catalyst at ammonia oxidation in the region of industrial application of the catalyst. A tubular reactor has been built for this purpose on whose internal side the active compound Co_3O_4 was fixed. The dependence of the outlet mixture composition on the wall temperature, feed

composition and feed rate was recorded. Also the temperature profile on the wall of the catalytic block was measured.

EXPERIMENTAL

Apparatus and Procedures

The measurements were performed with the mixture ammonia air with the content 3,5 and 10 mol% of ammonia and for the temperature ranges from 523 to 983 K. At each temperature the dependence of composition of the outlet mixture on flow rate was measured in the range from 50 to 428 l/h. The reaction mixture was prepared of pure compounds (NH_3) from the Chemical Works et Záluží, air from Technoplyn, Ostrava), which were taken from pressure flasks and were carried over columns with solid KOH and the molar sieve Nalsit 3A. The flow rate of pure

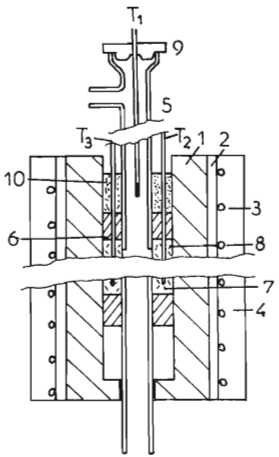

FIG. 1

Cross section through the reactor body. 1 External steel block, 2 layer of mica insulation, 3 resistance heater, 4 asbestos insulation, 5 quartz tube, 6 cementing mixture (TiO_2 + soluble glass), 7 block of the spinel Carrier, 8 thermocouple probes, 9 cap, 10 quartz sand, T_1, T_2, T_3 thermocouples

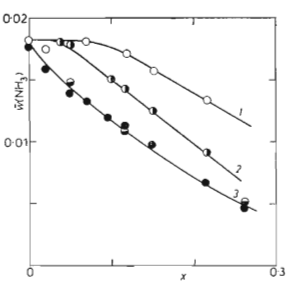

FIG. 2

Mean mass fraction of NH_3 in the outlet mixture w (NH_3) in dependence on axial coordinate x for air–ammonia mixture with 3% vol. of NH_3. *1* 523 K; *2* 623 K; *3* ◒ 923 K; ● 983 K

components was measured by capillary flowmeters. The control of flow rates was made by use of valves. The gaseous mixture was led from the mixer into the rotameter. Part of the gaseous mixture was taken to the analysis at the inlet into the rotameter. Flow rate of the mixture was controlled by use of valves. After passing through the reactor, part of products was led for an analysis and the rest was taken over the final manostate to the exhaust. Analyses of the inlet and outlet reaction mixture were performed chromatographically[37].

The body of the reactor was formed by a steel block (Fig. 1) with the outside diameter 20 mm into which was situated a cylinder of the catalytic material with the external diameter 11 mm and internal diameter 3 mm which was 64 mm long. In the catalyst, in parallel with the axis were drilled two holes of ID 0·7 mm, situated 2 mm from the internal wall of the cylinder and into the holes were fixed thermocouples T2, T3 NiCr (Walzwerk, Hettstedt). Into the cylinder of catalytic material were from both sides fixed quartz pipes whose ID was identical with the ID of the catalytic block. In the inlet pipe was situated a thermocouple for measurement of temperature of the fed reaction mixture (TI).

External wall of the steel block has been insulated by a layer of mica on which was wound the resistance heater. Whole body was thermally and electrically insulated from the environment by a layer of asbestos.

Catalyst Preparation

The catalyst was prepared by impregnation of the carrier by a solution of cobalt nitrate and by decomposition of the nitrate in the electric oven. The carrier was a mixture of 50% mass of Co_3O_4, 48% of α-alumina and 2% of TiO_2. This mixture has been homogenised in the ball mill and wetted. The formed body was treated into the form of cylinders with the diameters approximately 2 cm. So arranged carrier was annealed in the oven at 1 200°C for 8 h. After annealing, cylinders with the ED 11 mm were turned of the carrier and holes for thermocouples were drilled into them. So prepared cylindrical segments were twice impregnated at 130°C in a saturated solution of cobalt nitrate and were heated in the resistance oven to 400°C for half an hour. Into these cylinders, which were by a repeated impregnation relatively hard, were drilled holes on the walls of which was fixed catalytically active compound. So prepared carrier was eight times impregnated by saturated solution of $Co(NO_3)_2$ and after each impregnation the cobalt nitrate was decomposed at 600°C for half an hour. Temperature at the last two decompositions was increased to 800°C.

Cylindrical segments with the length 15 mm were ground on top faces into smooth planes and were bonded by the mixture of TiO_2 and water glass into blocks of the total length 64 mm.

The specific surface area of the so prepared catalyst was determined chromatographically[38] and was equal to 0·17 m^2/g. Porosity was determined by the mercury porosimeter (AG/65 Carlo Elba) and was 0·073 cm^3/g.

RESULTS AND DISCUSSION

The aim of the experiment was to obtain suitable data from which it would be possible to determine, by a method of nonlinear regression, kinetic parameters appearing in the boundary conditions of Eqs (*18*) and (*19*) of the last study[36]

$$(\partial\psi_i/\partial y)_{y=1} = Da_i \sum_k \alpha_{ki} \bar{R}_K \qquad (I)$$

$$\left(\frac{\partial \Theta}{\partial y}\right)_{y=1} = \sum_i \frac{Da_1}{Le_1} \delta_i \bar{R}_i + \beta_S \frac{\partial^2 \Theta_b}{\partial x^2} . \qquad (2)$$

Direct determination of surface concentrations of components was not possible, therefore the dependence of composition of the outlet mixture on temperature of the catalytic block, feed composition and flow rate of feed were measured. Also the temperature profile in the wall of the catalytic block was measured.

The measurements were performed with the mixture NH_3–air at three inlet concentrations of NH_3 (3%, 5%, and 10% mol NH_3) at temperatures 523 to 983 K. At each temperature was measured the dependence of composition of the outlet mixture on flow rate in the range from 50 to 428 l/h.

The measured mass fractions of NH_3, NO, N_2O and O_2 in the outlet mixture as function of the dimensionless coordinate are summarised in Figs 2 to 9.

Selection of the Reaction Scheme

At catalytic oxidation of ammonia by oxygen the products of oxidation are NO, N_2, N_2O. Composition of oxidation products is dependent on temperature of the catalyst and composition and flow rate of the reaction mixture. Survey of stoichiometric equations together with heats of reaction and values of equilibrium constants is given in Table I.

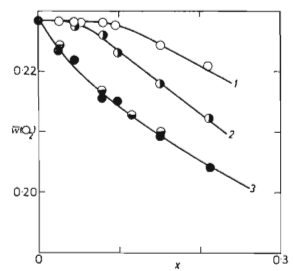

FIG. 3

Mean mass fraction of O_2 in the outlet mixture $w(O_2)$, in dependence on axial coordinate x for air–ammonia mixture with 3% vol. NH_3. *1* 523 K; *2* 623 K; *3* ◒ 923 K; ● 983 K

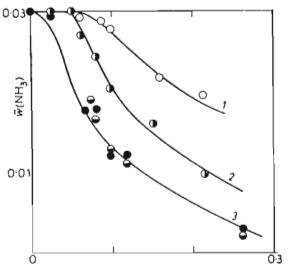

FIG. 4

Mean mass fraction of NH_3 in the outlet mixture $\bar{w}(NH_3)$ in dependence on axial coordinate x for air–ammonia mixture with 5% vol. of NH_3. *1* 523 K; *2* 623 K; *3* ◒ 923 K; ● 983 K

As results from the experiments at temperatures up to 350°C first of all reactions [2] and [3] are taking place, in the range from 400 to 600°C it is possible to expect formation of NO, N_2O and N_2 according to reactions [1], [2] and [3]. Above 700°C are the oxidation products only N_2 and NO.

For evaluation of experimental data the following reaction schemes haven been considered (numbers above the arrows correspond to numbering in Table I).

TABLE I

Summary of stoichiometric equations and their enthalpies and equilibrium constants[39]

Reaction	Stoichiometric equation	ΔH^0_{298}, kJ/mol NH_3	log K_{298}
{1}	$NH_3 + \frac{5}{4}O_2 = NO + \frac{3}{2}H_2O$	−226·51	44·26
{2}	$NH_3 + \frac{3}{4}O_2 = \frac{1}{2}N_2 + \frac{3}{2}H_2O$	−316·88	59·46
{3}	$NH_3 + O_2 = \frac{1}{2}N_2O + \frac{3}{2}H_2O$	−276·18	55·76
{4}	$NH_3 + \frac{3}{2}NO = \frac{5}{4}N_2 + \frac{3}{2}H_2O$	−452·45	82·25
{5}	$NH_3 + 4\,NO = \frac{5}{2}N_2O + \frac{3}{2}H_2O$	−474·23	101·74
{6}	$NH_3 + \frac{3}{2}N_2O = 2\,N_2 + \frac{3}{2}H_2O$	−444·50	86·63

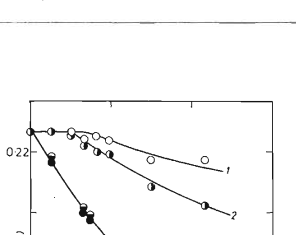

FIG. 5

Mean mass fraction O_2 in the outlet mixture $\bar{w}(O_2)$ in dependence on axial coordinate x air–ammonia mixture with 5% vol. NH_3. *1* 523 K; *2* 623 K; *3* ◒ 923 K; ● 983 K

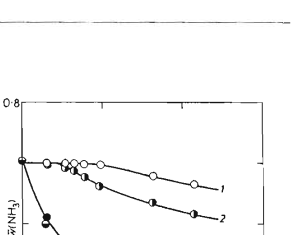

FIG. 6

Mean mass fraction of NH_3 in the outlet mixture $\bar{w}(NH)_3$ in dependence on axial coordinate x for air–ammonia mixture with 10% vol. NH_3. *1* 523 K; *2* 623 K; *3* ◓ 923K; ● 983 K

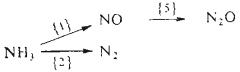

SCHEME 1

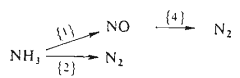

SCHEME 2

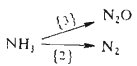

SCHEME 3

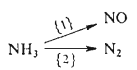

SCHEME 4

For expression of the dependence of reaction rate (R_i) on temperature and composition of the reaction mixture the empirical kinetic relations were used

$$R_i = k_i^0 \exp\left(-E_i/RT\right) \prod_j N_j^{\beta_{ij}}, \qquad (3)$$

where k_i^0 was the coefficient (mol m^{-2} s^{-1}), E_i apparent activation energy of the i-th reaction (J mol^{-1}), N_j mole fraction on the j-th component. β_{ij} order with respect to the j-th component in the i-th reaction.

By substitution of (*3*) into boundary conditions (*1*) and (*2*) together with the concrete stoichiometric matrix α_{ij} a system of nonlinear parabolic equations is obtained, whose solution gives the distribution of temperature ($\Theta(x, y)$) and composition ($\psi_i(x, y)$) and depends on kinetic parameters k_i^0, E_i, β_{ij} of relation (*3*). The final function whose minimum was searched for by the modified Rosenbrock method[39] was considered as the sum of square deviations of the calculated and measured value $\bar{\psi}_i$. The vector of composition of the outlet mixture $\bar{\psi}_i$ was obtained by integration of balance equations for individual components and energies by the method described in the last study[36]. Parameter β_s is a function of thermal conductivity of the solid phase λ_s which was taken as thermal conductivity of the pure γ-Al_2O_3 (ref.[40]) (6·7 W . . m^{-1} K^{-1})

Calculations

With regard to a relatively great number of serched parameters the order of individual components (matrix β_{ij}) in Eq. (3) was chosen as fixed. There were considered different combinations of the first and half order and by the optimisation procedure the parameter k_i^0, E_i were searched.

From the experimental data resulted that at temperatures up to 623 K are the products of ammonia oxidation only N_2 and NO. Therefore, the set of data has been divided into two parts which are further on denoted as I (523–623 K) and II (923 to 983 K). The transition region between 623 K and 923 K in which originate as products of oxidation N_2, N_2O and NO is not from the practical point of view significant and thus was not included into the regression calculation. For the set I were for evaluation of parameters of Eq. (3) used the Schemes 1 and 3 and for the set II the Schemes 2 and 4. The results of calculations are for different variants of the reaction order with respect to NH_3, O_2 and NO summarised in Tables II to III. With each variant is beside the calculated parameters E_i and k_i^0 given the standard deviation defined by relation

$$\text{standard deviation} = (\Phi(b^x)/(M - L))^{1/2}, \qquad (4)$$

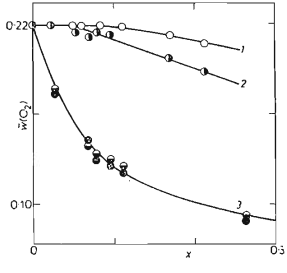

FIG. 7

Mean mass fraction of O_2 in the outlet mixture $\bar{w}(O_2)$ in dependence on axial coordinate x for air–ammonia mixture with 10% vol. *1* 523 K; *2* 623 K; *3* ◒ 923 K; ● 983 K

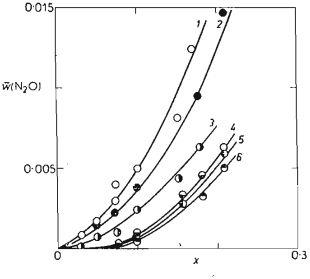

FIG. 8

Mean mass fraction of N_2O in the outlet mixture $\bar{w}(N_2O)$ in dependence on axial coordinate x for air–ammonia mixture with 3–10 vol. % NH_3, *1* 10 vol. % NH_3 523 K; *2* 5 vol. % NH_3 623 K; *3* 3 vol. % NH_3 623K; *4* 10 vol. % NH_3 523 K; *5* 5 vol. % NH_3 523 K; *6* 3 vol. % NH_3 523 K

where $\Phi(b^x)$ is the value of final function in the optimal point b^x, M is the number of experimental points and L the number of searched parameters.

In Figs 2 to 9 are given dependences of mass fractions or individual components as functions of the dimensionless coordinate $x = (z/r_0)/(Re \,.\, Pr)$.

Together with the calculated dependence are plotted also the experimentally determined values. For the set II (923 and 983 K) the theoretical values $\bar{w}_i^1$ were used in the calculation of the reaction scheme 2 with the parameters E_i, k_i^0 and β_{ij} of the variant 3 (Table II). For the set I (523 and 623 K) was used the reaction scheme 3, with the parameters E_i, k_i^0 and β_{ij} of the variant 3 (Table III). As results from Table III, the smallest standard deviation for the range of temperatures 523–623 K has the variant 3, to which correspond the rate equations in the form

$$r(N_2) = \tfrac{1}{2}9{\cdot}05 \,.\, 10^4 \exp\left(-78{\cdot}2/\boldsymbol{RT}\right) . N(NH_3) . N(O_2)\,, \tag{5}$$

$$r(N_2O) = \tfrac{1}{2}9{\cdot}2 \,.\, 10^2 \exp\left(-83{\cdot}5/\boldsymbol{RT}\right) . N(NH_3) . (N(O_2))^{0{\cdot}5}\,. \tag{6}$$

Similarly for the range of temperature 923–983 K from Table II the variant 3 has the best agreement of experimental data with the model

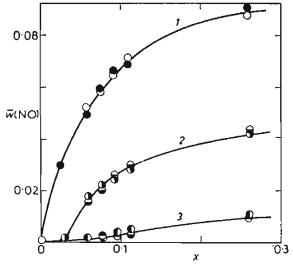

FIG. 9

Mean mass fraction of NO in the outlet mixture $\bar{w}$(NO) in dependence on axial coordinate x for air–ammonia mixture with 3,5 and 10 vol. % of NH_3. *1* 10 vol. % NH_3, ○ 923 K, ● 983 K; *2* 5 vol. % NH_3, ◑ 923 K, ◒ 983 K; *3* 3 vol. % NH_3, ◐ 923 K, ◓ 983 K

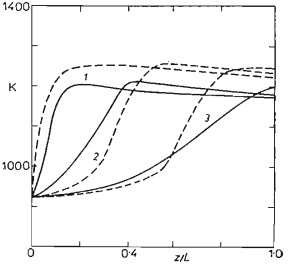

FIG. 10

Temperature of the wall in dependence on axial coordinate for 5 vol. % of NH_3. *1* 50 1/h, *2* 197 1/H, *3* 429 1/h. ——— Temperature measured by movable thermocouple; – – – – – temperature calculated from Eqs (*11*) and (*12*)

$$r(N_2) = \tfrac{1}{2}5{\cdot}1\,.\,10^3 \exp\left(-50{\cdot}2/\boldsymbol{RT}\right).\,N(NH_3).\,(N(O_2))^{0{\cdot}5} + \\ + \tfrac{5}{4}4{\cdot}5\,.\,10^3 \exp\left(-63{\cdot}4/\boldsymbol{RT}\right).\,N(NH_3).\,N(NO) \qquad (7)$$

TABLE II

Kinetic parameters for Schemes 1 and 2

Variant	Reaction	β_{ij}			E_i kJ/mol	k_i^0 $mol^{-1}\,s^{-1}\,m^{-2}$	Standard deviation
		NH_3	O_2	NO			
				Scheme 1 (set I)			
1	{1}	1	1	0	76·0	$7{\cdot}3\,.\,10^4$	
	{2}	1	1	0	62·7	$2{\cdot}3\,.\,10^2$	0·096
	{5}	1	0	1	38·6	$8{\cdot}0\,.\,10^5$	
2	{1}	0·5	1	0	71·8	$7{\cdot}5\,.\,10^4$	
	{2}	0·5	1	0	77·3	$3{\cdot}6\,.\,10^2$	0·23
	{5}	1	0	0·5	43·5	$7{\cdot}0\,.\,10^5$	
3	{1	1	0·5	0	85·5	$7{\cdot}0\,.\,10^4$	
	{2}	1	0·5	0	70·1	$3{\cdot}8\,.\,10^2$	0·024
	{5}	0·5	0	1	50·8	$6{\cdot}2\,.\,10^5$	
4	{1}	0·5	0·5	0	84·0	$7{\cdot}0\,.\,10^4$	
	{2}	0·5	0·5	0	61·0	$3{\cdot}6\,.\,10^2$	0·170
				Scheme 2 (set II)			
1	{1}	1	1	0	86·4	$7{\cdot}7\,.\,10^6$	
	{2}	1	1	0	46·2	$3{\cdot}0\,.\,10^3$	0·017
	{4}	1	0	1	65·0	$4{\cdot}6\,.\,10^3$	
2	{1}	0·5	1	0	74·1	$7{\cdot}9\,.\,10^6$	
	{2}	0·5	1	0	53·2	$4{\cdot}05\,.\,10^3$	0·024
	{4}	1	0	0·5	60·6	$5{\cdot}1\,.\,10^3$	
3	{1}	1	0·5	0	88·7	$7{\cdot}5\,.\,10^6$	
	{2}	1	0·5	0	50·2	$5{\cdot}1\,.\,10^3$	0·012
	{4}	1	0	1	63·4	$4{\cdot}5\,.\,10^3$	
4	{1}	0·5	0·5	0	83·2	$7{\cdot}6\,.\,10^6$	
	{2}	0·5	0·5	0	55·1	$5{\cdot}8\,.\,10^3$	0·150
	{4}	0·5	0	0·5	58·7	$3{\cdot}2\,.\,10^3$	

$$r(\mathrm{NO}) = 7{\cdot}5 \,.\, 10^6 \exp\left(-88{\cdot}7/\boldsymbol{RT}\right) . N(\mathrm{NH_3}) . (N(\mathrm{O_2}))^{0.5} - \\ - \tfrac{3}{2}4{\cdot}5 \,.\, 10^3 \exp\left(-63{\cdot}4/\boldsymbol{RT}\right) . N(\mathrm{NH_3}) . N(\mathrm{NO}) . \qquad (8)$$

CONCLUSIONS

At comparison of calculated and measured temperature profiles on the wall of the reactor it has been demonstrated that the agreement of result is only qualitative

TABLE III
Kinetic parameters for Schemes 3 and 4

Variant	Reaction	β_{ij}		E_i kJ/mol	k_i^0 $\mathrm{mol^{-1}\ s^{-1}\ m^{-2}}$	Standard deviation
		NH_3	O_2			
				Scheme 3 (set I)		
1	{2}	1	1	74·6	$8{\cdot}2 \,.\, 10^4$	
	{3}	1	1	88·7	$8{\cdot}0 \,.\, 10^2$	0·076
2	{2}	0·5	1	56·4	$9{\cdot}0 \,.\, 10^5$	
	{3}	0·5	1	92·2	$7{\cdot}4 \,.\, 10^2$	0·032
3	{2}	1	1	78·2	$9{\cdot}05 \,.\, 10^4$	
	{3}	1	0·5	83·5	$9{\cdot}2 \,.\, 10^2$	0·010
4	{2}	0·5	0·5	72·0	$6{\cdot}6 \,.\, 10^4$	
	{3}	0·5	0·5	86·6	$1{\cdot}05 \,.\, 10^3$	0·088
				Scheme 4 (set II)		
1	{1}	1	1	96·3	$1{\cdot}05 \,.\, 10^7$	
	{2}	1	1	50·1	$2{\cdot}5 \,.\, 10^4$	0·852
2	{1}	0·5	1	78·5	$1{\cdot}7 \,.\, 10^7$	
	{2}	0·5	1	52·4	$2{\cdot}4 \,.\, 10^4$	0·532
3	{1}	1	0·5	80·7	$1{\cdot}9 \,.\, 10^7$	
	{2}	1	0·5	56·0	$3{\cdot}2 \,.\, 10^4$	0·105
4	{1}	0·5	0·5	85·8	$2{\cdot}8 \,.\, 10^7$	
	{2}	0·5	0·5	59·2	$4{\cdot}0 \,.\, 10^4$	0·233

(Fig. 10). As is demonstrated by the presented example the model is capable to demonstrate the effect of the magnitude of feed rate on the formed profile and also predict the sharp temperature increase of the wall in the point of transfer of reaction into the region of external diffusion.

The differences of calculated and experimental values of the wall temperature can be the result of the used technique of temperature measurement and by the effect not included in the mathematical model. The movable thermocouple is equipped with a jacket made of stainless steel thus there can occur a distortion of the measured temperature by axial heat conduction in the thermocouple probe. As is demonstrated in the study[41] the temperature difference between the wall surface and the thermocouple does not exceed 10 K.

As the most significant effects which are not respected by the mathematical model and which can significantly affect the wall temperature is the radiation heat transfer[42] and changes in transport quantities (μ, D_i, λ_g) with temperature and composition of the reaction mixture.

Critical evaluation of these effects in a concrete case is rather difficult and is the topic of the following study.

LIST OF SYMBOLS

A_s cross sectional area of the catalytic block (m^2)
C_p thermal capacity of the gaseous mixture at constant pressure ($J\ kg^{-1}\ K^{-1}$)
D_i effective diffusion coefficient of component i ($m^2\ s^{-1}$)
Da_i Damköhler number
E_i activation energy of the i-th reaction ($kJ\ mol^{-1}$)
$\bar{G}$ density vector of total mass flux ($kg\ m^{-2}\ s^{-1}$)
k_i^0 term in Eq. (3) ($mol\ m^{-2}\ s^{-1}$)
L length of reactor (m)
Le_i Lewis number
N_j mole fraction of j-th component
N_i molecular mass of the i-th component ($kg\ mol^{-1}$)
Pr Prandtl number
r^9 radius of pipe (m)
$\bar{R}_k$ dimensionsless reaction rate of the k-th reaction
R_i reaction rate of the i-th reaction ($mol\ m^{-2}\ s^{-1}$)
r_i rate of formation or consumption of the i-th component ($mol\ m^{-2}\ s^{-1}$)
Re Reynolds number
V_0 volumetric flow rate of the reaction mixture related to 293 K and 101 325 Pa
x dimensionless axial coordinate
y dimensionless radial coordinate
z axial coordinate (m)
α_{ij} matrix of stoichiometric coefficients
β_{ij} reaction order with respect to the j-th component in the i-th reaction
$\beta_s = A_s\lambda_s/2\pi\lambda r_0^2(Re\ Pr)^2$

δ_i dimensionless adiabatic increase in temperature of the i-th reaction
Θ dimensionless temperature of the gaseous phase
Θ_b dimensionless temperature of the solid phase
λ_g thermal conductivity of the gaseous mixture ($J\,m^{-1}\,s^{-1}\,K^{-1}$)
μ dynamic viscosity of gaseous mixture ($kg\,m^{-1}\,s^{-1}$)
ϱ density of mixture ($kg\,m^{-3}$)
ψ_i relative mass fraction of the i-th component
$\bar{\psi}_i$ mean mixing cup value of ψ_i

REFERENCES

1. Atroshchenko V. I., Kargin S. I.: *Tekhnologia Azotnoi Kisloty* 3rd Ed., p. 77. Khimiia Moscow 1970.
2. Andrussow L.: Z. Angew. Chem. *39*, 321 (1926).
3. Andrussow L.: Z. Angew. Chem. *41*, 205 (1928).
4. Andrussow L.: Z. Angew. Chem. *41*, 262 (1928).
5. Andrussow L.: Z. Angew. Chem. *63*, 350 (1951).
6. Andrissow L.: Bull. Soc. Chem. Fr. *1*, 981 (1951).
7. Andrussow L.: Bull. Soc. Chim. Fr. *1*, 45 (1951).
8. Bodenstein M.: Z. Angew. Chem. *40*, 174 (1927).
9. Bodenstein M.: Z. Angew. Chem. *47*, 364 (1934).
10. Bodenstein M.: Trans. Electrochem. Soc. *71*, 20 (1937).
11. Bodenstein M.: Z. Electrochem. *47*, 501 (1941).
12. Krauss W.: Z. Phys. Chem. (Leipzig) *B39*, 83 (1938).
13. Krauss W.: Z. Phys. Chem. (Leipzig) *B39*, 1 (1939).
14. Krauss W.: Z. Phys. Chem. (Leipzig) *54*, 264 (1950).
15. Zawadski J.: Discuss. Faraday Soc. *8*, 140 (1950).
16. Rashig F.: Z. Angew. Chem. *40*, 1183 (1927).
17. Rashig F.: Z. Angew. Chem. *41*, 265 (1928).
18. Kučera J.: Chem. Listy *69*, 1142 (1974).
19. Fogel J. M.: Kinet. Katal. *5*, 496 (1964i.
20. Nutt C. W., Kapur S.: Nature (London) *224*, 169 (1969).
21. Nutt C. W., Kapur S.: Nature (London) *220*, 697 (1968).
22. Pignet T., Schmidt L. D.: Chem. Eng. Sci. *29*, 1123 (1974).
23. Pignet T., Schmidt L. D.: J. Catal. *40*, 212 (1975i.
24. Morrow B. A., Cody I. A.: J. Catal. *45*, 151 (1976).
25. Ostermaier J. J., Latzer J. R., Manoque W. H.: J. Catal. *33*, 457 (1974).
26. Ostermaier J. J.: Katzer J. R., Manoque W. H.: J. Catal. *41*, 277 (1976).
27. Ilchenko I. I., Golodec G. I.: Kinet. Katal. *15*, 394 (1974).
28. Ilchenko I. I., Golodec G. I.: J. Catal. *39*, 57 (1975).
29. Grifiths D. W., Hallam H. E., Thomas W. J.: J. Catal. *17*, 18 (1970).
30. Barelko V. V., Volodin J. E.: Dokl. Akad. Nauk SSSR *211*, 1373 (1973).
31. Barelko V. V., Volodin J. E.: Dokl. Akad. Nauk SSSR *216*, 1080 (1974).
32. Barelko V. V., Volodin J. E.: Kinet. Katal. *17*, 118 (1976).
33. Barelko V. V., Volodin J. E.: Kinet. Katal. *17*, 683 (1976).
34. Šub F. S., Chomenko A. A., Apelbaum L. O., Temkin L. I.: Kinet. Katal. *17*, 157 (1976).
35. Countor J. P., Mouvier G., Hoogewys M., Leclere C.: J. Catal. *48*, 217 (1977).
36. Bernauer B., Šimeček A., Vosolsobě J.: This Journal, in press.
37. Bernauer B., Šimeček A., Vosolsobě J.: Chem. Prům. *28*, 515 (1978).

38. Nielsen F. M., Eggertsen F. T.: Anal. Chem. *30*, 1937 (1958).
39. Himmelblau D. M.: *Applied Nonlinear Programming*. McGraw-Hill, New York 1972.
40. *International Critical Tables*, Vol. V., p. 216. McGraw-Hill, New York 1927.
41. Lee S., Aris R.: Chem. Eng. Sci. *32*, 827 (1977).
42. Bernauer B.: *Thesis*. Prague Institute of Chemical Technology, Prague 1978.

Translated by M. Rylek.